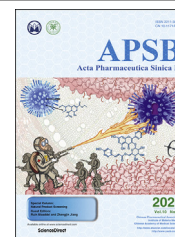




Chinese Pharmaceutical Association
Institute of Materia Medica, Chinese Academy of Medical Sciences

Acta Pharmaceutica Sinica B

www.elsevier.com/locate/apsb
www.sciencedirect.com



SHORT COMMUNICATION

Impact of molecular weight on the mechanism of cellular uptake of polyethylene glycols (PEGs) with particular reference to P-glycoprotein



Tingting Wang^{a,c}, Yingjie Guo^c, Yang He^d, Tianming Ren^c, Lei Yin^a,
John Paul Fawcett^c, Jingkai Gu^{b,c,e,*}, Huimin Sun^{f,*}

^aClinical Laboratory, First Hospital, Jilin University, Changchun 130061, China

^bResearch Institute of Translational Medicine, First Hospital, Jilin University, Changchun 130061, China

^cResearch Center for Drug Metabolism, College of Life Science, Jilin University, Changchun 130012, China

^dDepartment of Pharmaceutical Sciences and Experimental Therapeutics, College of Pharmacy, University of Iowa, Iowa City IA 52242, USA

^eBeijing Institute of Drug Metabolism, Beijing 102209, China

^fNational Institutes for Food and Drug Control, Beijing 100050, China

Received 25 December 2019; received in revised form 15 January 2020; accepted 1 February 2020

KEY WORDS

P-gp;
PEGs;
P-gp-substrate;
Passive diffusion;
Endocytosis

Abstract Polyethylene glycols (PEGs) in general use are polydisperse molecules with molecular weight (MW) distributed around an average value applied in their designation *e.g.*, PEG 4000. Previous research has shown that PEGs can act as P-glycoprotein (P-gp) inhibitors with the potential to affect the absorption and efflux of concomitantly administered drugs. However, questions related to the mechanism of cellular uptake of PEGs and the exact role played by P-gp has not been addressed. In this study, we examined the mechanism of uptake of PEGs by MDCK-mock cells, in particular, the effect of MW and interaction with P-gp by MDCK-hMDR1 and A549 cells. The results show that: (a) the uptake of PEGs by MDCK-hMDR1 cells is enhanced by P-gp inhibitors; (b) PEGs stimulate P-gp ATPase activity but to a

Abbreviations: ACN, acetonitrile; AUC, area under the plasma concentration-time curve; CE, collision energy; C_{max} , maximum plasma concentration; CsA, cyclosporine A; DBD, drug-binding domain; DDS, drug delivery system; DMEM, Dulbecco's modified Eagle's medium; DMSO, dimethyl sulfoxide; DP, declustering potential; FBS, fetal bovine serum; HBSS, Hanks' balanced salt solution; HEPES, 4-(2-hydroxyethyl)-1-piperazineethanesulfonic acid; IS, internal standard; LC–HRMS/MS, liquid chromatography–high resolution tandem mass spectrometry; MW, molecular weight; NBD, nucleotide binding domain; PAC, paclitaxel; PEG, polyethylene glycol; P-gp, P-glycoprotein; VER, verapamil.

*Corresponding authors. Tel: +86 431 88155381; fax: +86 431 88155380 (Jingkai Gu). Tel: +86 10 67095721; fax: +86 10 67052750 (Huimin Sun).

E-mail addresses: gujuk@jlu.edu.cn (Jingkai Gu), sunhm@nifdc.org.cn (Huimin Sun).

Peer review under responsibility of Institute of Chinese Pharmaceutical Association and Institute of Materia Medica, Chinese Academy of Medical Sciences.

<https://doi.org/10.1016/j.apsb.2020.02.001>

2211-3835 © 2020 Chinese Pharmaceutical Association and Institute of Materia Medica, Chinese Academy of Medical Sciences. Production and hosting by Elsevier B.V. This is an open access article under the CC BY-NC-ND license (<http://creativecommons.org/licenses/by-nc-nd/4.0/>).

much lesser extent than verapamil; and (c) uptake of PEGs of low MW (<2000 Da) occurs by passive diffusion whereas uptake of PEGs of high MW (>5000 Da) occurs by a combination of passive diffusion and caveolae-mediated endocytosis. These findings suggest that PEGs can engage in P-gp-based drug interactions which we believe should be taken into account when using PEGs as excipients and in PEGylated drugs and drug delivery systems.

© 2020 Chinese Pharmaceutical Association and Institute of Materia Medica, Chinese Academy of Medical Sciences. Production and hosting by Elsevier B.V. This is an open access article under the CC BY-NC-ND license (<http://creativecommons.org/licenses/by-nc-nd/4.0/>).

1. Introduction

PEGs in general use are polydisperse molecules applied as excipients to improve solubility and dissolution of pharmaceuticals. They are also used to form conjugates with drug molecules (PEGylation) and to prepare PEGylated drug delivery systems (DDS), such as liposomes and nanoparticles^{1–3}. When PEGs or PEGylated therapeutics are ingested, recipients are inevitably exposed to free PEG^{4,5}. This is generally considered to have little clinical significance, but there are reports of free PEGs causing adverse effects due to their tendency to accumulate in tissues⁶ and acting as P-gp inhibitors^{7–9}. This paper reports the results of a study into the mechanism of cellular uptake of PEGs with different molecular weight (MW) and the role played by P-gp in the process.

P-gp is a membrane protein that acts as an important mediator of drug efflux from cells¹⁰ through possession of a drug-binding domain (DBD) and a nucleotide binding domain (NBD)^{11,12}. P-gp substrates first bind to the DBD after ATP hydrolysis at the NBD by ATPase, which provides the energy to bring about efflux¹³. Some P-gp inhibitors also act in this way but others can act by directly inhibiting ATPase¹⁴. Given that a molecule must be hydrophobic in order to enter the binding pocket of the DBD, PEGs are generally considered to be too hydrophilic to act as P-gp substrates and, to date, there is no evidence that they can. In addition, while PEGs can act as P-gp inhibitors, it remains unclear whether this is due to their ability to inhibit ATPase or to an indirect mechanism involving the disruption of the cell membrane in which P-gp is embedded⁹.

Using two novel bioanalytical methods based on liquid chromatography–high resolution tandem mass spectrometry (LC–HRMS/MS) developed in our laboratory¹⁵, we investigated the cellular uptake of polydisperse PEGs both as total PEG concentration and as a profile of each individual PEG homolog. This allowed us to determine the effect of MW and illuminate the role of P-gp. We believe the results increase our understanding of the fate and potential toxicity of PEGs when administered as excipients, PEGylated drugs and PEGylated DDS^{16,17} in the future design and clinical use of PEG therapeutics.

2. Materials and methods

2.1. Materials

Materials were supplied as follows: colchicine (purity 98.5%), chlorpromazine (purity > 88%), genistein (purity > 98%), quercetin (purity > 85%) and verapamil (VER, purity > 99 %) (Dalian

Meilun Biotechnology Company, Dalian, China); simvastatin (purity >99.8%) for use as internal standard (IS, National Institute for the Control of Pharmaceutical and Biological Products, Beijing, China); cyclosporine A (CsA, purity > 98.5%) and methoxy polyethylene glycol (PEG) 750, 2000, 5000 and 20,000 (Sigma–Aldrich, St. Louis, MO, USA); MDCK-hMDR1 and MDCK-mock (P-gp knockdown) cells at passage number 5–15 (Prof. Su Zeng, College of Pharmaceutical Sciences, Zhejiang University, Hangzhou, China); A549 cells (the American Type Culture Collection, Rockville, MD, USA); Dulbecco's modified Eagle's medium (DMEM), fetal bovine serum (FBS) and trypsin (Gibco, Grand Island, NY, USA); Hanks' balanced salt solution (HBSS), 4-(2-hydroxyethyl)-1-piperazine ethanesulfonic acid (HEPES) and penicillin-streptomycin solution (Dingguo Changsheng Biotechnology Company, Beijing, China); HPLC grade acetonitrile (ACN, Fisher Scientific, Pittsburgh, PA, USA); BCA protein assay kit (Pierce, Rockford, IL, USA); Pgp-GLO™ Assay System (Promega, Madison, WI, USA). All other chemicals were of analytical grade and used as received. Ultrapure water was prepared using the Milli-Q system (Millipore, Billerica, MA, USA).

2.2. Cell culture

Cells were grown in DMEM with 10% FBS, 1% nonessential amino acid solution and 1% penicillin-streptomycin solution in 75 cm² plastic culture flasks (Nunc, Roskilde, Denmark) at 37 °C in a humidified atmosphere containing 5% CO₂.

2.3. PEG uptake by MDCK-hMDR1, MDCK-mock and A549 cells

All drugs were dissolved in DMSO and subsequently diluted in transport buffer [HBSS containing 10 mmol/L HEPES (pH 7.4)]. PEGs were dissolved and diluted in transport buffer. Cells were seeded on 6-well plates (6 × 10⁴ cells/cm²). Medium was changed every two days and experiments were conducted after 5 days in culture.

To study the effect of P-gp inhibitors on cell uptake of PEGs, MDCK-hMDR1 cells were preincubated (0.5 h) and incubated (2 h) at 37 °C as follows: (1) preincubation with transport buffer followed by incubation with PEG (25 and 50 μmol/L, control); (2) preincubation with VER (200 μmol/L) followed by incubation with VER (200 μmol/L) and PEG (25 and 50 μmol/L) together; and (3) preincubation with CsA (10 μmol/L) followed by incubation with CsA (10 μmol/L) and PEG (25 and 50 μmol/L) together.

To investigate the MW dependence of PEG uptake into MDCK-mock cells, MDCK-mock cells were incubated with PEG 750 (50, 100, 500 and 1000 $\mu\text{mol/L}$) or PEGs 2000, 5000 or 20,000 (5, 10, 50 and 100 $\mu\text{mol/L}$) at 37 °C and 4 °C for 2 h.

To further investigate the mechanism of uptake of low MW PEGs, A549 cells were incubated at 37 °C with PEG 750 or 2000 (50 $\mu\text{mol/L}$) for various lengths of time up to 24 h. To further investigate the mechanism of uptake of high MW PEGs, MDCK-mock cells were preincubated (0.5 h) and incubated (2 h) as follows: (1) preincubation with transport buffer followed by incubation with PEG 5000 or 20,000 (100 $\mu\text{mol/L}$) at 37 °C (positive control); (2) preincubation with transport buffer followed by incubation with PEG 5000 or 20,000 (100 $\mu\text{mol/L}$) at 4 °C (negative control); (3) preincubation with colchicine (40 $\mu\text{g/mL}$) followed by incubation with colchicine (40 $\mu\text{g/mL}$) and PEG at 37 °C; (4) preincubation with chlorpromazine (10 $\mu\text{g/mL}$) followed by incubation with colchicine (10 $\mu\text{g/mL}$) and PEG at 37 °C; (5) preincubation with genistein (50 $\mu\text{g/mL}$) followed by incubation with genistein (50 $\mu\text{g/mL}$) and PEG at 37 °C; (6) preincubation with quercetin (100 $\mu\text{g/mL}$) followed by incubation with quercetin (100 $\mu\text{g/mL}$) and PEG at 37 °C^{18,19}.

After incubations, cells were processed as previously reported²⁰. In brief, cells were: (1) rinsed 3 times with ice-cold transport buffer, (2) collected using a cell scraper, (3) ultrasonicated, (4) centrifuged at 9000 \times g, 4 °C for 30 min (to remove the cell fragment and organelle) and (5) the protein and intracellular PEG concentration determined. Intracellular PEG concentrations are given in ng/ μg protein.

2.4. Determination of PEGs in cell lysates

LC was based on our previously reported method¹⁵ with modifications to improve peak shape. A 50 μL aliquot of sample was mixed with 20 μL IS solution (1 $\mu\text{g/mL}$ in ACN) and 150 μL cold ACN (-20 °C) after which samples were centrifuged at

15,000 rpm (ThermoPico17-A, Thermo Fisher Scientific, Waltham, MA, USA) for 5 min and 50 μL supernatant analyzed. Chromatographic conditions for assay of the different PEGs are listed in Table 1.

HRMS/MS utilized the MS^{ALL} technique in which PEG precursor ions are dissociated to fragments in the collision cell. The MS parameters for assay of all PEGs were as follows: declustering potential (DP) and collision energy (CE) were 100 V and 30 eV, respectively; nebulizer, heater and curtain gas flow rates (N_2) were 50, 50 and 30 psi, respectively; ionspray needle voltage was 5500 V; heater gas temperature was 500 °C. Quantitation was conducted by extracting the product ions of PEGs and IS in the m/z ranges of 133.06–133.10 and 225.16–225.17, respectively. Data acquisition and integration was controlled by Analyst TF version 1.7.1 software. Representative LC–HRMS chromatograms and mass spectra are provided in Supporting Information.

2.5. Effect of PEGs on P-gp ATPase activity

P-gp ATPase activity was estimated using the P-gp-Glo assay system according to the manufacturer's instructions²⁰. Briefly, human P-gp overexpressing membranes were incubated with PEGs (25 and 50 $\mu\text{mol/L}$), VER (200 $\mu\text{mol/L}$), Na_3VO_4 (100 $\mu\text{mol/L}$) or buffer alone in a 96-well plate for 5 min. Mg-ATP was added to initiate the reaction (40 min). ATP Detection Reagent (Pgp-GLOTM Assay System, Promega, Madison, WI, USA) was added (20 min) to assay the residual ATP content. ATP consumption was detected as a decrease in luminescence, the less ATP remaining, the higher the P-gp ATPase activity was²¹.

2.6. MW profiling of uptake of PEGs 750 and 2000 by A549 cells

After incubation of A549 cells with PEGs, a 50 μL aliquot of cell lysate was mixed with 200 μL ACN, the mixture centrifuged at

Table 1 Analytical conditions for analyzing of total PEG concentration and each individual PEG homolog.

Analyte	Chromatography column	Column temperature (°C)	Solvent A	Solvent B	Gradient program	Flow rate (mL/min)
PEG 750	Zorbax 300SB-C18 column (150 mm \times 4.6 mm, 5 μm , 300 Å, Agilent)	40	0.1% Formic acid in water	ACN	0–1 min 10% B; 1–3 min 10%–90% B; 3–5.5 min 90% B; 5.5–5.6 min 90%–10% B; 5.6–8 min 10% B	0.6
PEG 2000 PEG 5000	Zorbax 300SB-C18 column (150 mm \times 4.6 mm, 5 μm , 300 Å, Agilent)	40	0.1% Formic acid in water	ACN	0–1 min 20% B; 1–5 min 20%–95% B; 5–7.9 min 95% B; 7.9–8 min 95%–20% B; 8–10 min 20% B	
PEG 20,000	PLRP-S column (50 mm \times 4.6 mm, 8 μm , 1000 Å, Agilent)	55	0.1% Formic acid in water	ACN:isopropanol (50:50)	0–1 min 20% B; 1–4.5 min 20%–80% B; 4.5–6.9 min 80% B; 6.9–7 min 80%–20% B; 7–9 min 20% B	
MW profiling	Zorbax 300SB-C18 column (150 mm \times 4.6 mm, 5 μm , 300 Å, Agilent)	30	0.1% Formic acid in water	0.1% Formic acid ACN	0–1 min 17% B; 1–10 min 17%–30% B; 10–22 min 30%–33% B; 22–24 min 33%–80% B; 24–26 min 80% B; 26–26.1 min 80%–17% B; 26.1–30 min 17% B	0.8

15,000 rpm (ThermoPico17-A, Thermo Fisher Scientific) for 5 min and 50 μL supernatant removed for analysis. The chromatographic conditions for this study are listed in Table 1. Detection by Q-Q-TOF MS was as described in Section 2.4. Except that the CE was reduced to 10 eV to ensure all PEG precursor ions entered Q2 intact. Data are presented as peak areas (cps) of individual homologs divided by the protein concentration acting as IS. Standard solutions of PEGs were prepared by spiking control cell lysate. Representative LC–HRMS/MS chromatograms and mass spectra for this study are provided in Supporting Information.

3. Results and discussion

3.1. Effect of P-gp inhibitors on PEG uptake by MDCK-hMDR1 cells

Previous studies have shown that free PEGs can act as P-gp inhibitors *in vitro*^{8,9,22}. In our preliminary study, PEG was shown to affect the pharmacokinetics (PK) of the P-gp substrate, paclitaxel (PAC), in rat *in vivo* (Supporting Information Table S2 and Fig. S3). The large interindividual variability in plasma concentration–time curves is probably due to variability in the expression of P-gp and CYP3A, and the low oral absorption of PAC²³. The maximum plasma concentration (C_{max}) and area under the plasma concentration–time curve (AUC) in the PEG pre-treated group is higher than in control. This result is consistent with a previous study showing that PEG 400 can alter the bioavailability of other P-gp substrates²⁴. To date there are no reports relating to whether PEGs can act as P-gp substrates yet.

P-gp substrates are expected to accumulate in P-gp over-expressing cells in the presence of P-gp inhibitors. To investigate whether PEGs are effluxed by P-gp, we incubated the P-gp overexpressing MDCK-hMDR1 cell line with PEGs concentrations of around 40 $\mu\text{mol/L}$ (the reported concentration of PEG 2000 in rats after intravenous injection of PEGylated doxorubicin⁵ in the presence of VER and CsA (P-gp substrates and competitive inhibitors). The results shown in Fig. 1 reveal that the uptake of PEGs by MDCK-hMDR1 cells is significantly increased in the presence of VER and to an even greater extent in the presence of CsA. This is consistent with the known greater affinity of CsA for P-gp²⁵. The results clearly indicate that PEGs can be effluxed by P-gp.

3.2. Effect of PEGs on P-gp ATPase activity

P-gp-mediated efflux of P-gp substrates leads to activation of P-gp ATPase and increasing consumption of ATP²⁶. To seek further evidence that PEGs are P-gp substrates, we applied the P-gp-Glo assay system to determine the consumption of ATP by P-gp in the presence of PEGs. It was found that VER significantly reduced the content of ATP whereas Na_3VO_4 (a non-competitive inhibitor of P-gp ATPase) significantly increased it²⁰. This is consistent with the above results showing that VER stimulates P-gp ATPase directly while Na_3VO_4 inhibits it indirectly by binding to other sites in P-gp such as the ATP binding site. PEGs, like VER, decreased the content of ATP, albeit to a much lesser extent (Fig. 2), indicating that PEGs, like VER, bind to the P-gp DBD and activate P-gp ATPase. The fact that the efflux of PEGs is inhibited by VER and CsA and that PEGs increase the activity of P-gp ATPase are consistent with previous research¹² suggesting

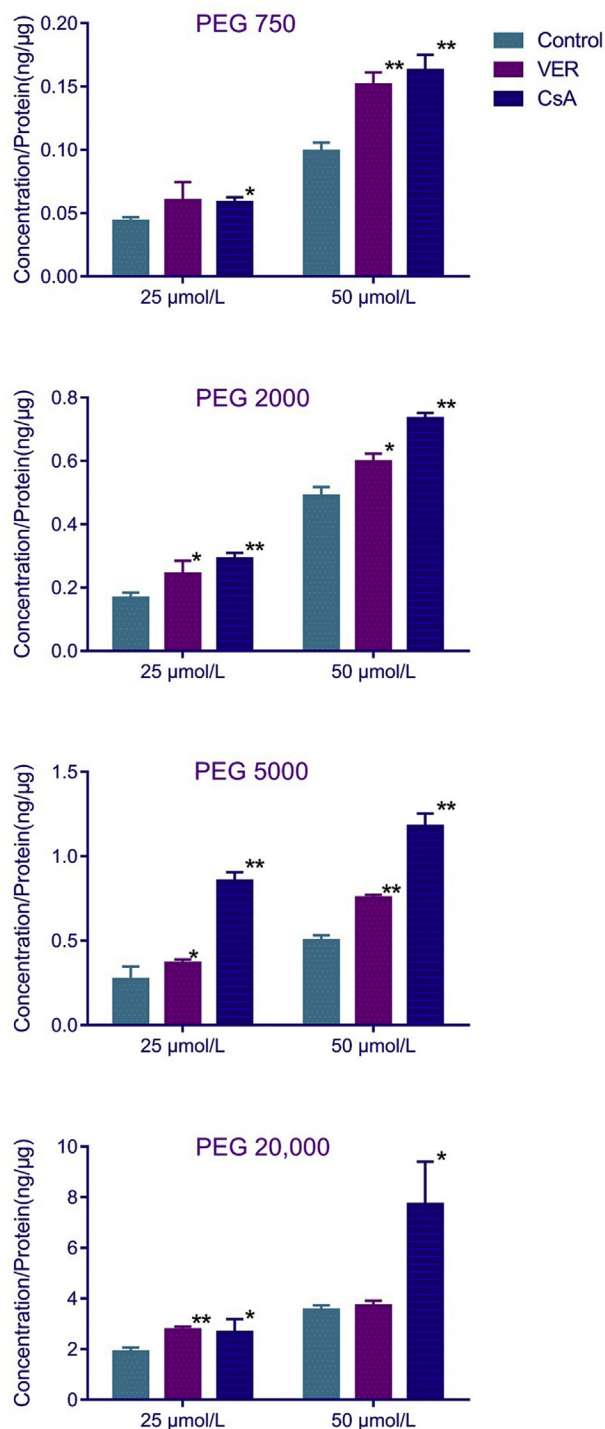


Figure 1 Effects of VER and CsA on the uptake of PEGs with different MW by MDCK-hMDR1 cells. Cells were preincubated with transport buffer (1) alone (control) or (2) containing VER (200 $\mu\text{mol/L}$) or (3) containing CsA (10 $\mu\text{mol/L}$) for 0.5 h. After removal of medium, cells were incubated with corresponding solutions containing PEGs (25 or 50 $\mu\text{mol/L}$) for 2 h. Total intracellular PEG concentration (ng/ μg protein) was determined by LC–Q-Q-TOF MS using with MS^{ALL} technique and are means \pm SD of three independent experiments. * $P < 0.05$ vs. control, ** $P < 0.01$ vs. control.

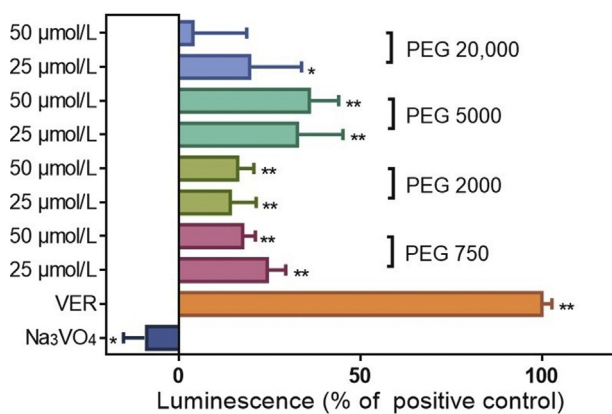


Figure 2 Effect of PEGs on P-gp ATPase activity in the P-gp-Glo assay system. Human P-gp overexpressing membranes of the P-gp-Glo™ Assay System were incubated with either PEGs, Na_3VO_4 (negative control) or VER (positive control). Residual ATP content was detected by luminescence and is expressed relative to the difference between positive control and untreated control set at 100%. Data are means \pm SD of 4 independent experiments. * $P < 0.05$ vs. untreated control; ** $P < 0.01$ vs. untreated control.

that PEGs have the same binding site on P-gp (the DBD) as VER and CsA. The weak stimulation of ATPase activity produced by PEG 20,000 is discussed in Section 3.3.

3.3. PEG uptake by MDCK-mock cells

Whenever a nanoparticle produced by self-assembly of a PEGylated drug encounters a cell, it is rapidly taken up through endocytosis²⁷. However, given that PEGs alone do not readily form nanoparticles, this pathway of PEG uptake may not or only apply to PEGs with relatively high MW. Since endocytosis and P-gp efflux require energy, they can be eliminated by incubating cells at low temperature (4 °C) unlike passive diffusion which is not affected by temperature²⁸. However, given the possibility that P-gp could influence the comparison of PEG uptake at 4 °C and at 37 °C, we used P-gp knockdown MDCK-mock cells to avoid this potential complication.

The intracellular concentrations of PEG 750 after incubation with 5 or 10 $\mu\text{mol/L}$ were too low to be detected, and therefore required higher concentrations (50, 100, 500 and 1000 $\mu\text{mol/L}$) than used for PEGs 2000, 5000 and 20,000 (5, 10, 50 and 100 $\mu\text{mol/L}$). The concentration and temperature dependence of the uptakes of PEGs are shown in Fig. 3 which also shows the proportion of PEGs entering cells by passive diffusion (the ratio of uptake at 4 °C to that at 37 °C). The results show that the uptakes of PEGs 750 and 2000 increase linearly with concentration and are not affected by temperature indicating they occur by passive diffusion^{28–30}. This result is surprising given that PEGs are amphiphilic polymers that are generally considered to be with limited cellular uptake³¹. PEGs 5000 and 20,000 behaved similarly at concentrations $< 10 \mu\text{mol/L}$, but, at concentrations $> 50 \mu\text{mol/L}$, uptake was greater at 37 °C than at 4 °C. Furthermore, when the concentration increased from 50 to 100 $\mu\text{mol/L}$, the proportion of PEGs 5000 and 20,000 entering cells by passive diffusion decreased from 84.6% to 54.0% and 63% to 47%, respectively. This is speculated to arise because PEGs 5000 and 20,000 tend to aggregate at higher concentrations causing a higher

proportion of their uptake to occur by endocytosis^{27,32,33}. Aggregation may also explain the weak stimulation of ATPase activity produced by PEG 20,000 which is much weaker at

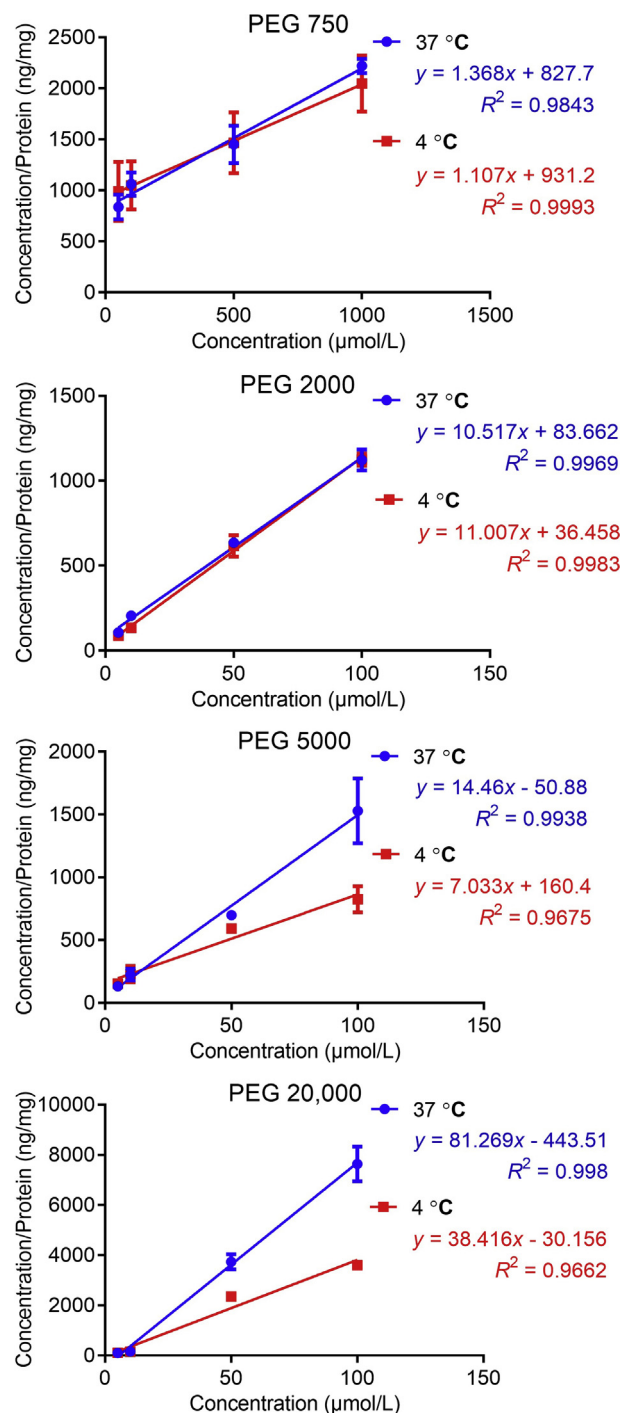


Figure 3 The uptake of PEGs 750, 2000, 5000 and 20,000 by MDCK-mock cells over 2 h as a function of concentration and temperature. Cells were incubated in transport buffer containing PEG 750 (50, 100, 500 or 1000 $\mu\text{mol/L}$) or PEGs 2000, 5000 or 20,000 (5, 10, 50 or 100 $\mu\text{mol/L}$) at 37 °C and 4 °C. Total intracellular PEG concentration (ng/mg protein) was determined by LC-Q-Q-TOF MS using the MS^{ALL} technique and are the means of three independent experiments. Percentages indicate the proportion of uptake by passive diffusion (uptake at 4 °C:uptake at 37 °C).

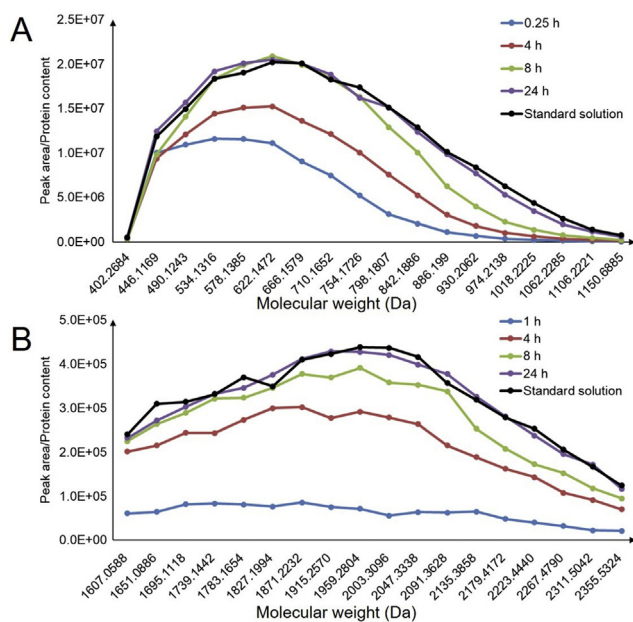


Figure 4 MW profile of uptake of (A) PEG 750 and (B) PEG 2000 by A549 cells as a function of duration of incubation. Cells were incubated with PEGs 750 or 2000 (50 $\mu\text{mol/L}$) in transport buffer at 37 $^{\circ}\text{C}$. Individual PEG homologs in A549 cells were analyzed by LC–Q–Q–TOF MS as parent ions without fragmentation and are presented as peak areas (cps) divided by the protein concentration acting as IS. Standard solutions of PEGs were prepared by spiking control cell lysate and analyzed in the same way. Data are means \pm SD of three independent experiments.

50 $\mu\text{mol/L}$ than at 25 $\mu\text{mol/L}$. Because the proportion of PEG 5000 entering cells by passive diffusion at 50 $\mu\text{mol/L}$ is 84.6%, the stimulation of ATPase activity at 50 $\mu\text{mol/L}$ is not significantly less than at 25 $\mu\text{mol/L}$.

3.4. MW profiling of PEG uptake by A549 cells

Because PEGylated drugs are mainly used to treat cancer, we chose A549 non-small cell lung cancer cells to examine the MW profiles of PEG 750 and 2000 uptake as a function of duration of incubation. The results for the different time intervals in Fig. 4 show that PEG 2000 enters cells more slowly than PEG 750 as its homologs are only detected after 1 h. Fig. 4 also shows that uptake of the lower MW homologs in PEG 750 (the PEG with the lower average MW) is more rapid than uptake of the higher MW homologs such that, after 0.25 h, the MW profile is skewed towards lower MW. In contrast, uptake of PEG 2000 is much slower and, even after 1 h, gives a profile that shows no evidence of being skewed to low MW. However, by 24 h, both profiles resemble those of the corresponding standard solutions.

3.5. Uptake of high MW PEGs by endocytosis

The results described above reveal that low MW PEGs (750 and 2000) enter cells by passive diffusion with no contribution from endocytosis whereas high MW PEGs enter cells by a combination of passive diffusion and endocytosis. To further investigate the mechanism of uptake of high MW PEGs by endocytosis, MDCK-mock cells were incubated with PEGs 5000 and 20,000 in the presence of the endocytosis inhibitors,

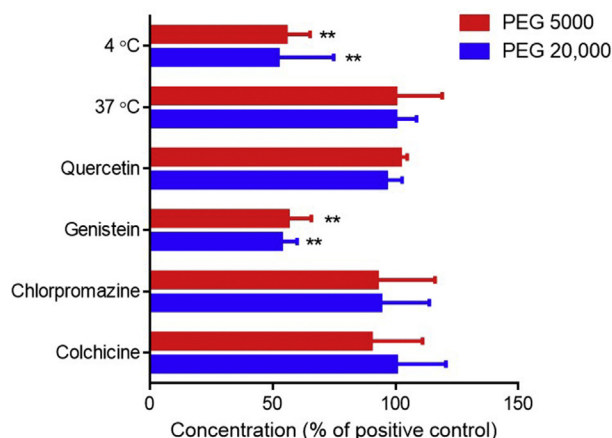


Figure 5 Effects of colchicine, chlorpromazine, genistein and quercetin on the uptake of PEGs 5000 and 20,000 by MDCK-mock cells. Cells were preincubated in transport buffer (1) alone (positive control) at 37 $^{\circ}\text{C}$, (2) alone (negative control) at 4 $^{\circ}\text{C}$, containing (3) colchicine (40 $\mu\text{g/mL}$), (4) chlorpromazine (10 $\mu\text{g/mL}$), (5) genistein (50 $\mu\text{g/mL}$) or (6) quercetin (100 $\mu\text{g/mL}$) for 0.5 h. After removal of medium, cells were incubated in corresponding solutions containing PEGs (100 $\mu\text{mol/L}$) for 2 h. Total intracellular PEG concentration (ng/mg protein) was determined by LC–Q–Q–TOF MS using the MS^{ALL} technique and expressed relative to the positive control set at 100%. Data are means \pm SD of three independent experiments. ** $P < 0.01$ vs. positive control.

colchicine (an inhibitor of micropinocytosis), chlorpromazine (an inhibitor of clathrin-mediated endocytosis), genistein (an inhibitor of caveolae-mediated endocytosis) and quercetin (an inhibitor of caveolae- and clathrin-independent endocytosis). MDCK-mock cells were used because all the inhibitors of endocytosis (colchicine³⁴, chlorpromazine³⁵, genistein³⁶ and quercetin^{36,37}) are also inhibitors of P-gp and therefore avoid this complication in studying the role of endocytosis in the uptake of PEGs. As shown in Fig. 5, the uptakes of PEGs 5000 and 20,000 are significantly lower at 4 $^{\circ}\text{C}$ and in the presence of genistein compared to positive control but are not significantly different in the presence of the other inhibitors. This suggests that PEGs 5000 and 20,000 enter cells mainly through the caveolae-mediated endocytosis pathway.

4. Conclusions

PEGs are polydisperse polymers widely used as excipients and in PEGylated drug conjugates and DDS. Despite their hydrophilic nature, there is some evidence that PEGs can access cells and interact with P-gp, but how this occurs is unknown. The results of this study show that PEGs are indeed taken up by cells and act as P-gp substrates. PEGs with relatively low MW (average 750 and 2000 Da) cross cell membranes by passive diffusion whereas those with higher MW (average 5000 and 20,000 Da) enter cells by a combination of passive diffusion and caveolae-mediated endocytosis at higher concentration. In terms of the intracellular MW profile of PEGs entering by passive diffusion, lower MW homologs are taken up more rapidly. We maintain these results have important implications in the pharmaceutical and clinical use of PEGs.

Acknowledgments

The authors thank Professor Su Zeng, College of Pharmaceutical Sciences, Zhejiang University, Hangzhou, China, for kindly providing MDCK-hMDR1 and MDCK-mock cells. This work was supported by grants from the National Natural Science Foundation of China (Grant Nos. 81430087, 81673396, 81872831 and 81603182), and the National Science and Technology Major Projects for 'significant new drugs creation' of the 13th five-year plan (2017ZX09101001 and 2018ZX09721002007, China).

Author contributions

Jingkai Gu and Huimin Sun participated in research design. Tingting Wang, Yingjie Guo, Tianming Ren and Lei Yin conducted experiments. Tingting Wang and Yang He performed data analysis. Tingting Wang and John Paul Fawcett wrote or contributed to the writing of the manuscript.

Conflicts of interest

The authors declare there are no conflicts of interest. This work did not involve studies with human subjects.

Appendix A. Supporting information

Supporting data to this article can be found online at <https://doi.org/10.1016/j.apsb.2020.02.001>.

References

- Herzberger J, Niederer K, Pohlit H, Seiwert J, Worm M, Wurm FR, et al. Polymerization of ethylene oxide, propylene oxide, and other alkylene oxides: synthesis, novel polymer architectures, and bioconjugation. *Chem Rev* 2015;**116**:2170–243.
- Vilasaliu D, Fowler R, Stolnik S. PEGylated nanomedicines: recent progress and remaining concerns. *Expert Opin Drug Deliv* 2014;**11**: 139–54.
- Li C, Wang J, Wang Y, Gao H, Wei G, Huang Y, et al. Recent progress in drug delivery. *Acta Pharm Sin B* 2019;**9**:1145–62.
- Lin W, Yin L, Sun T, Wang T, Xie Z, Gu J, et al. The effect of molecular structure on cytotoxicity and antitumor activity of PEGylated nanomedicines. *Biomacromolecules* 2018;**19**:1625–34.
- Yin L, Su C, Ren T, Meng X, Shi M, Fawcett JP, et al. MS^{All} strategy for comprehensive quantitative analysis of PEGylated-doxorubicin, PEG and doxorubicin by LC-high resolution q-q-TOF mass spectrometry coupled with all window acquisition of all fragment ion spectra. *Analyst* 2017;**142**:4279–88.
- Longley CB, Zhao H, Lozanguiez YL, Conover CD. Biodistribution and excretion of radiolabeled 40 kda polyethylene glycol following intravenous administration in mice. *J Pharm Sci* 2013;**102**: 2362–70.
- Johnson BM, Charman WN, Porter CJH. An *in vitro* examination of the impact of polyethylene glycol 400, pluronic P85, and vitamin E d- α -tocopheryl polyethylene glycol 1000 succinate on P-glycoprotein efflux and enterocyte-based metabolism in excised rat intestine. *AAPS PharmSci* 2002;**4**:193–205.
- Hugger ED, Novak BL, Burton PS, Audus KL, Borchardt RT. A comparison of commonly used polyethoxylated pharmaceutical excipients on their ability to inhibit P-glycoprotein activity *in vitro*. *J Pharm Sci* 2002;**91**:1991–2002.
- Shen Q, Lin Y, Handa T, Doi M, Sugie M, Wakayama K, et al. Modulation of intestinal P-glycoprotein function by polyethylene glycols and their derivatives by *in vitro* transport and *in situ* absorption studies. *Int J Pharm (Amst)* 2006;**313**:49–56.
- Silva R, Vilas-Boas V, Carmo H, Dinis-Oliveira RJ, Carvalho F, de Lourdes Bastos M, et al. Modulation of P-glycoprotein efflux pump: induction and activation as a therapeutic strategy. *Pharmacol Therapeut* 2015;**149**:1–123.
- Zhou M, Li L, Li L, Lin X, Wang F, Li Q, et al. Overcoming chemotherapy resistance *via* simultaneous drug-efflux circumvention and mitochondrial targeting. *Acta Pharm Sin B* 2019;**9**:615–25.
- Chufan EE, Sim HM, Ambudkar SV. Molecular basis of the poly-specificity of P-glycoprotein (ABCB1): recent biochemical and structural studies. *Adv Cancer Res* 2015;**125**:71–96.
- Mollazadeh S, Sahebkar A, Hadizadeh F, Behravan J, Arabzadeh S. Structural and functional aspects of P-glycoprotein and its inhibitors. *Life Sci* 2018;**214**:118–23.
- Ziyad B, Afsaneh L. P-glycoprotein inhibition as a therapeutic approach for overcoming multidrug resistance in cancer: current status and future perspectives. *Curr Cancer Drug Targets* 2013;**13**: 326–46.
- Zhou X, Meng X, Cheng L, Su C, Sun Y, Sun L, et al. Development and application of an MS^{All}-based approach for the quantitative analysis of linear polyethylene glycols in rat plasma by liquid chromatography triple-quadrupole/time-of-flight mass spectrometry. *Anal Chem* 2017;**89**:5193–200.
- Nieto Montesinos R, Beduneau A, Pellequer Y, Lamprecht A. Delivery of P-glycoprotein substrates using chemosensitizers and nanotechnology for selective and efficient therapeutic outcomes. *J Contr Release* 2012;**161**:50–61.
- Iyer AK, Singh A, Ganta S, Amiji MM. Role of integrated cancer nanomedicine in overcoming drug resistance. *Adv Drug Deliv Rev* 2013;**65**:1784–802.
- Xu X, Sabanayagam CR, Harrington DA, Farach-Carson MC, Jia X. A hydrogel-based tumor model for the evaluation of nanoparticle-based cancer therapeutics. *Biomaterials* 2014;**35**:3319–30.
- Boylan NJ, Kim AJ, Jung Soo S, Pichet A, Simons BW, Lai SK, et al. Enhancement of airway gene transfer by DNA nanoparticles using a pH-responsive block copolymer of polyethylene glycol and poly-L-lysine. *Biomaterials* 2012;**33**:2361–71.
- Wang T, Sun Y, Ma W, Yang Z, Yang J, Liu J, et al. Trantinterol, a novel beta2-adrenoceptor agonist, noncompetitively inhibits P-glycoprotein function *in vitro* and *in vivo*. *Mol Pharm* 2015;**12**:1–9.
- Ambudkar SV, Dey S, Hrycyna CA, Ramachandra M, Pastan I, Gottesman MM. Biochemical, cellular, and pharmacological aspects of the multidrug transporter. *Annu Rev Pharmacol* 1999;**39**: 361–98.
- Ashiru-Oredope DA, Patel N, Forbes B, Patel R, Basit AW. The effect of polyoxyethylene polymers on the transport of ranitidine in Caco-2 cell monolayers. *Int J Pharm (Amst)* 2011;**409**:164–8.
- de Weger VA, Beijnen JH, Schellens JHM. Cellular and clinical pharmacology of the taxanes docetaxel and paclitaxel—a review. *Anti-cancer Drug* 2014;**25**:488–94.
- Mai Y, Afonso-Pereira F, Murdan S, Basit AW. Excipient-mediated alteration in drug bioavailability in the rat depends on the sex of the animal. *Eur J Pharmaceut Sci* 2017;**107**:249–55.
- Hsiao P, Unadkat JD. Predicting the outer boundaries of P-glycoprotein (P-gp)-based drug interactions at the human blood–brain barrier based on rat studies. *Mol Pharm* 2014;**11**:436–44.
- Palmeira A, Sousa E, Vasconcelos MH, Pinto MM. Three decades of P-gp inhibitors: skimming through several generations and scaffolds. *Curr Med Chem* 2012;**19**:1946–2025.
- Sun T, Zhang YS, Pang B, Hyun DC, Yang M, Xia Y. Engineered nanoparticles for drug delivery in cancer therapy. *Angew Chem Int Ed* 2014;**53**:12320–64.
- Pisani MJ, Fromm PD, Mulyana Y, Clarke RJ, Körner H, Heimann K, et al. Mechanism of cytotoxicity and cellular uptake of lipophilic inert dinuclear polypyridylruthenium (II) complexes. *ChemMedChem* 2011;**6**:848–58.
- Novohradsky V, Liu Z, Vojtiskova M, Sadler PJ, Brabec V, Kasparikova J. Mechanism of cellular accumulation of an iridium(III)

- pentamethylcyclopentadienyl anticancer complex containing a C, N-chelating ligand. *Metall* 2014;**6**:682–90.
30. Price KA, Crouch PJ, Volitakis I, Paterson BM, Lim S, Donnelly PS, et al. Mechanisms controlling the cellular accumulation of copper bis (thiosemicarbazonato) complexes. *Inorg Chem* 2011;**50**:9594–605.
 31. D'souza AA, Shegokar R. Polyethylene glycol (PEG): a versatile polymer for pharmaceutical applications. *Expet Opin Drug Deliv* 2016;**13**:1257–75.
 32. Shang L, Nienhaus K, Nienhaus GU. Engineered nanoparticles interacting with cells: size matters. *J Nanobiotechnol* 2014;**12**:5.
 33. Verma A, Uzun O, Hu Y, Han HS, Watson N, et al. Surface-structure-regulated cell-membrane penetration by monolayer-protected nanoparticles. *Nat Mater* 2008;**7**:588–95.
 34. Dahan A, Sabit H, Amidon GL. Multiple efflux pumps are involved in the transepithelial transport of colchicine: combined effect of p-glycoprotein and multidrug resistance-associated protein 2 leads to decreased intestinal absorption throughout the entire small intestine. *Drug Metab Dispos* 2009;**37**:2028–36.
 35. Brown D, Goosen TC, Chetty M, Hamman JH. Effect of oral contraceptives on the transport of chlorpromazine across the Caco-2 intestinal epithelial cell line. *Eur J Pharm Biopharm* 2003;**56**:159–65.
 36. Jaganathan SK. Can flavonoids from honey alter multidrug resistance?. *Med Hypotheses* 2011;**76**:535–7.
 37. Wang SY, Duan KM, Li Y, Mei Y, Sheng H, Liu H, et al. Effect of quercetin on P-glycoprotein transport ability in Chinese healthy subjects. *Eur J Clin Nutr* 2013;**67**:390–4.